

$7^2D_{3/2}$ - $7^2D_{5/2}$ excitation transfer in rubidium induced in collisions with ground-state Rb and noble-gas atoms

J. Wolnikowski,* J. B. Atkinson, J. Supronowicz, and L. Krause

Department of Physics, University of Windsor, Windsor, Ontario N9B 3P4, Canada

(Received 9 November 1981)

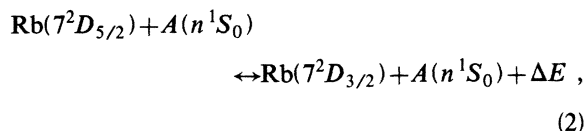
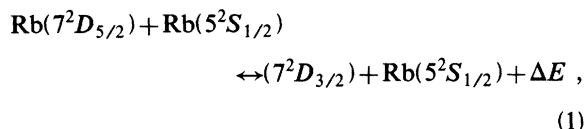
Cross sections for $7^2D_{3/2} \leftrightarrow 7^2D_{5/2}$ transfer in Rb, induced in collisions with He, Ne, Ar, and with ground-state Rb atoms, have been determined using methods of atomic fluorescence. Rb vapor, pure or mixed with a noble gas, was irradiated in a glass fluorescence cell with pulses of 660-nm radiation from a N_2 -laser-pumped dye laser, populating one of the 2D states by two-photon absorption. The resulting fluorescence included a direct component emitted in the decay of the optically excited state and a sensitized component arising from the collisionally populated state. Relative intensities of the components yielded the cross sections for 7^2D mixing: $Q(^2D_{3/2} \rightarrow ^2D_{5/2}) = 8.8, 6.5, 10.4,$ and 30 ; $Q(^2D_{3/2} \leftarrow ^2D_{5/2}) = 5.8, 4.0, 6.9,$ and 18 , in units of 10^{-14} cm^2 for He, Ne, Ar, and Rb, respectively. Cross sections for the effective quenching of the 2D states were also determined.

I. INTRODUCTION

Excitation transfer between highly excited states of alkali-metal atoms continues to be the subject of numerous investigations. Experimental studies of such processes induced by collisions with noble-gas atoms were carried out for sodium by Biraben *et al.*¹ and by Gallagher *et al.*² For rubidium such processes were studied by Hugon *et al.*^{3,4} They determined cross sections for quenching of the states $9F-21F$, $9D-15D$, and $12S-18S$, and also for transfer between fine-structure states induced by helium collisions for the states $9D-13D$. Theoretical calculations of cross sections for the quenching of n^2D and n^2F alkali Rydberg states were carried out by Prunelé and Pascale⁵ and more general theories dealing with collisions of atoms in Rydberg states have been developed by Omont⁶ and Hahn.⁷ Collisions of atoms excited to states between the resonance and "true" Rydberg states are also of considerable interest but not many of them have been studied. Experimental measurements of cross sections for excitation transfer between fine-structure components have been reported for Rb 6^2P , 7^2P and Cs 7^2P (Ref. 8) as well as Rb 8^2D (Ref. 9) states which are not encompassed by most of the theoretical treatments.

In this paper, we are reporting the results of an experimental investigation of the transfer between the $7^2D_{3/2}$ and $7^2D_{5/2}$ states in rubidium, induced in collisions with ground-state Rb, He, Ne, and Ar atoms. Excitation transfer between these states

may be represented as follows:



where A denotes a noble-gas atom and $\Delta E = 1.51 \text{ cm}^{-1}$ is the energy defect between the $7D_{3/2}$ and $7D_{5/2}$ states.

When Rb atoms are selectively excited to one of the 2D fine-structure states, its decay to the $5P_{1/2}$ or $5P_{3/2}$ state results in the emission of fluorescent light. Before decaying, some of the primarily excited atoms undergo inelastic collisions causing their transfer to the other 2D fine-structure state whose decay gives rise to the emission of sensitized fluorescence. Collisions of excited Rb atoms in the 2D state may also cause radiationless transfer to other lower-energy states, resulting in a depopulation of the 2D states and manifested as an overall quenching effect. Since electric dipole transitions between the 2S and 2D states are forbidden, an indirect method had to be used to populate the 7^2D fine-structure states. Various methods have been reported elsewhere, such as stepwise excitation by way of the resonance state,¹⁰ cascade transitions from higher states,¹¹ as well as two-photon absorp-

tion.⁹ The latter method was chosen since it could be easily put into effect using an available dye laser.

II. THE EXCITATION AND DECAY PROCESSES

A partial energy-level diagram for rubidium, showing the states involved in the experiment as well as the transitions between them, is shown in Fig. 1. The $7D_{3/2}$ or $7D_{5/2}$ state is selectively excited by two-photon absorption using a tunable dye laser. The fluorescence resulting from the decay of the $7D$ states can be spectrally isolated with a monochromator so that only transitions between the $7D$ and $5P$ states need be considered. The $7D_{5/2}$ state may decay spontaneously only to the $5P_{3/2}$ state, while the $7D_{3/2}$ state may decay either to the $5P_{1/2}$ or to the $5P_{3/2}$ state. The $5P_{1/2}$ - $5P_{3/2}$ separation is 238 cm^{-1} and is easily resolved, but the fine-structure splitting of the $7D$ state is 1.51 cm^{-1} and could not be resolved with the available monochromator. Consequently, the observed fluorescent spectrum consists of two components, one at 572.4 nm and the other at 564.8 nm . When the $7D_{5/2}$ state is optically excited, the

572.4-nm component of both direct and sensitized fluorescence, while the 564.8-nm component is entirely due to sensitized fluorescence. When, on the other hand, the $7D_{3/2}$ state is the primarily excited state, the 564.8-nm component is entirely due to direct fluorescence, whereas the 572.4-nm component consists of a mixture of direct and sensitized fluorescence. The proportions of direct and sensitized fluorescence present in each spectral component may be calculated, though when $D_{3/2}$ is the primarily excited state, there is an effective lower limit to the noble-gas or Rb vapor densities, in order that the relative intensity of the sensitized fluorescence in the 572.4-nm component be at least comparable to the intensity of the direct fluorescence. On the other hand, when the primarily excited state is the $D_{5/2}$ state, there is no such limitation because the component at 564.8 nm is due entirely to sensitized fluorescence.

When the $7^2D_{3/2}$ is optically excited [Fig. 1(a)], the density of the collisionally populated $7^2D_{5/2}$ state may be represented by the rate equation

$$\frac{dN_4}{dt} = N_3 N_0 v Q_{34} - N_4 \left[\frac{1}{\tau_4} + N_0 v Q_{43} + N_0 v Q_4 \right]. \quad (3)$$

In the reverse case [Fig. 1(b)]

$$\frac{dN_3}{dt} = N_4 N_0 v Q_{43} - N_3 \left[\frac{1}{\tau_3} + N_0 v Q_{34} + N_0 v Q_3 \right], \quad (4)$$

where τ and N are lifetimes and population densities of states indicated by the subscripts 1,2,3,4, corresponding to $5^2P_{1/2}$, $5^2P_{3/2}$, $7^2D_{3/2}$, and $7^2D_{5/2}$, respectively. N_0 is the density of the colliding partner atoms, which may be ground-state Rb or noble-gas atoms. Q_{34} and Q_{43} are the total (thermally averaged) cross sections for transfers $7^2D_{3/2} \rightarrow 7^2D_{5/2}$ and $7^2D_{5/2} \rightarrow 7^2D_{3/2}$, respectively, while Q_3 and Q_4 are the cross sections for effective quenching—collisional transfer to all other Rb states; $v = (8kT/\pi\mu)^{1/2}$ is the average relative speed of the colliding partners whose reduced mass is μ .

Although the populations of the 2D states are time dependent because of pulsed excitation, Eqs. (3) and (4) can be integrated to give¹²

$$\frac{\bar{N}_3}{\bar{N}_4} = \frac{1}{\tau_4 Q_{34}} \frac{1}{N_0 v} + \frac{Q_{43} + Q_4}{Q_{34}}, \quad (5)$$

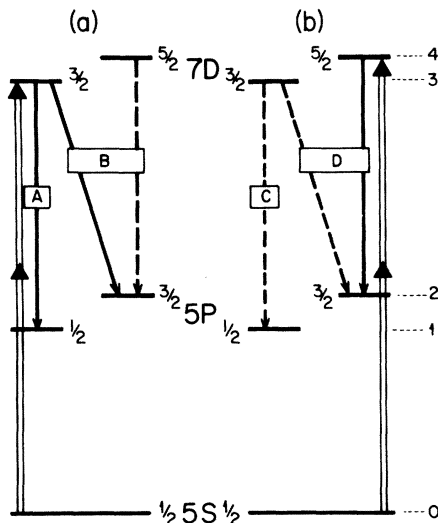


FIG. 1. A partial energy-level diagram showing the Rb states involved in the two-photon absorption and fluorescent emission processes. Part (a) indicates the transitions which take place when the $7^2D_{3/2}$ state is optically excited, part (b) corresponds to optical excitation of the $7^2D_{5/2}$ state (diagram not to scale). The observed fluorescent components labeled A, B, C, D, have the following wavelengths: $\lambda_A = \lambda_C = 564.8\text{ nm}$; $\lambda_B = \lambda_D = 572.4\text{ nm}$.

$$\frac{\bar{N}_4}{\bar{N}_3} = \frac{1}{\tau_3 Q_{43}} \frac{1}{N_0 \nu} + \frac{Q_{34} + Q_3}{Q_{43}}. \quad (6)$$

In Eq. (5) \bar{N}_4 represents the time-integrated population produced by collisional excitation transfer, whereas \bar{N}_3 is due to optical excitation; in Eq. (6) the reverse is the case. Assuming the measured fluorescent intensities to be proportional to the products of the appropriate populations and Einstein A coefficients, Eqs. (5) and (6) may be expressed in terms of the time-integrated intensities of the spectral components A , B , C , and D :

$$\frac{1}{I_B/I_A - (A_{32}/A_{31})} = \frac{A_{31}}{A_{42}} \frac{1}{\tau_4 Q_{34}} \frac{1}{N_0 \nu} + \frac{A_{31}}{A_{32}} \frac{Q_{43} + Q_4}{Q_{34}}, \quad (7)$$

$$\frac{I_D}{I_C} = \frac{A_{42}}{A_{31}} \frac{1}{\tau_3 Q_{43}} \frac{1}{N_0 \nu} + \frac{A_{42}}{A_{31}} \frac{Q_{34} + Q_3}{Q_{43}} + \frac{A_{32}}{A_{31}}. \quad (8)$$

The lifetimes τ_3 and τ_4 were assumed equal to one another and were calculated from transition probabilities quoted by Anderson and Zilitis,¹³ which yielded a value of 397 ns, close to recent experimental results.^{14,15} The ratios of A coefficients were calculated from oscillator strengths given by Migdalek and Baylis.¹⁶ They are $A_{32}/A_{31} = 0.2106$ and $A_{42}/A_{31} = 1.2524$.

III. EXPERIMENTAL

A schematic arrangement of the apparatus is shown in Fig. 2. The exciting radiation was emitted by a N_2 -laser-pumped dye laser and, after attenuation by a neutral-density filter, was brought to a focus inside the fluorescence cell mounted in an oven and containing either pure Rb vapor or a mixture of Rb vapor with a noble gas. The resulting fluorescence emitted at right angles to the direction of excitation was analyzed with a monochromator and registered with a photon counter whose output was displayed by a printer.

The dye laser, which was set up in a Littmann double-grating configuration,¹⁷ employed a magnetically stirred dye cell containing a mixture of Rhodamine 6G and Cresyl Violet Perchlorate dyes. It produced light pulses of 5-ns duration at a repetition rate of 25 Hz in the 660-nm wavelength band. The spectral width of the emitted light, which was monitored with a Fabry-Perot etalon, was about 5

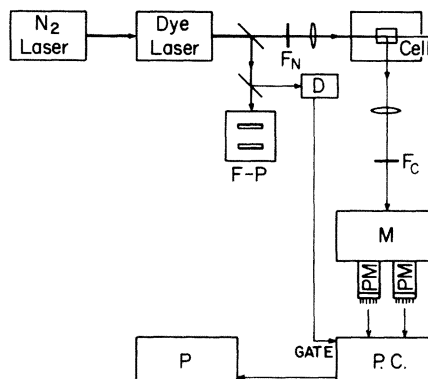


FIG. 2. Schematic diagram of apparatus. M is the monochromator, PM the photomultiplier tubes, PC the photon counter, P the printer, F-P the Fabry-Perot etalon, D the photodiode, F_N the neutral density filter, and F_C the color filter.

GHz and was very much smaller than the separation of the 7^2D fine-structure substates which amounted to 45.3 GHz (1.51 cm^{-1}). Since the excitation took place by two-photon absorption, the effective spectral width of the exciting radiation was 2×5 GHz, exceeding considerably the width of the absorption lines. We have verified that the 2^2D states were indeed excited selectively since, when the dye laser was tuned to a frequency midway between the two states, neither was observed to be populated.

The fluorescence cell which was made of Pyrex glass, was cylindrical in shape, 4-cm long, and 2.5 cm in diameter. It has a sidearm 7-cm long and 1 cm in diameter, which was located below the body of the cell and contained liquid rubidium metal. The cell was also connected to a vacuum and gas-filling system through a greaseless stopcock mounted inside the oven, which allowed the cell to be evacuated and filled with variable gas pressures while preventing the loss of rubidium from the cell. The oven was heated electrically and had a separately thermostated jacket surrounding the sidearm, through which silicone oil was circulated from an ultrathermostat. Natural rubidium (supplied by Metron, Inc. of Allamuchy, N. J.) of 99.9% nominal purity was redistilled under vacuum and then distilled into the sidearm of the cell which had previously been baked out for several days at a temperature of over 400°C and a vacuum of about 10^{-8} Torr. The sidearm temperature which determined the Rb vapor pressure in the cell

was maintained constant within ± 0.2 K and was kept about 30 K below the cell temperature to prevent condensation on the windows. Temperatures were measured by several copper-Constantan thermocouples attached to the cell and sidearm. The saturated vapor pressure of rubidium was calculated from the (lowest) sidearm temperature and the usual temperature-vapor pressure relations.¹⁸ During the experiments with pure rubidium, the sidearm temperature was varied in the interval 393–460 K which corresponded to a pressure range 1–30 mTorr. In the measurements with the noble gases, "research grade", supplied by Union Carbide Linde Gas Products, we used a Rb vapor pressure of 4×10^{-5} Torr to reduce to a minimum the effects of Rb-Rb collisions.

The half-meter grating monochromator which was used to analyze the fluorescence, was equipped with two exit slits which permitted the simultaneous detection of the two spectral components at 564.8 nm and 572.4 nm by two RCA C31034 photomultipliers whose outputs were registered by the two channels of an Ortec 9315 photon counter preceded by two 9302 amplifier discriminators. The photon counter was gated on by the laser pulses, each of which activated the counter for a time span equivalent to about 10 lifetimes of the excited states, resulting in a considerable reduction of the background noise. The simultaneous recording of the intensities of both spectral components of the fluorescence also reduced errors arising from fluctuations in the intensity of the laser light. The relative sensitivities of the two detection and counting channels, which had to be known for the determination of the collision cross sections, were measured using an auxiliary Rb spectral lamp for which the relative intensities of the spectral lines were measured using each photomultiplier and photon counter separately. An additional check was carried out using a calibrated halogen standard light source. The fluorescent light was also examined for polarization and was found to be almost completely depolarized.⁹

At the beginning of each experimental run, the system was baked and pumped to a vacuum of 10^{-8} Torr. Noble-gas pressures were measured using an autovac gauge and a trapped McLeod gauge. The gas pressures were varied from about 1 mTorr to over 100 mTorr, above which the ratio of sensitized to direct fluorescence became insensitive to further changes in gas pressure. The pressures were corrected for transpiration where appropriate.

IV. RESULTS AND DISCUSSION

Equations (7) and (8) may be written

$$\frac{A_{42}}{A_{31}} \left(\frac{I_B}{I_A} - \frac{A_{32}}{A_{31}} \right)^{-1} = \frac{1}{\tau} \frac{1}{Q_{34}} C \frac{\sqrt{T}}{P} + \frac{Q_{34} + Q_4}{Q_{34}}, \quad (9)$$

$$\frac{A_{31}}{A_{42}} \left(\frac{I_D}{I_C} - \frac{A_{32}}{A_{31}} \right) = \frac{1}{\tau} \frac{1}{Q_{43}} C \frac{\sqrt{T}}{P} + \frac{Q_{34} + Q_3}{Q_{43}}, \quad (10)$$

where $C = \sqrt{\pi k \mu / 8}$ and P is the total pressure in the cell. When the transitions are induced by collisions with ground-state Rb atoms, P represents the Rb vapor pressure.

Figure 3 shows plots of Eqs. (9) and (10) against \sqrt{T}/P for pure Rb vapor. As expected, the graphs are linear; their slopes yield the cross sections Q_{34} and Q_{43} and the intercepts give the effective quenching cross sections Q_3 and Q_4 . The values Q_{34} and Q_{43} which are listed in Table I are considered to be accurate within $\pm 15\%$, the main sources of error arising from the uncertainty in the determination of the vapor pressures from sidearm

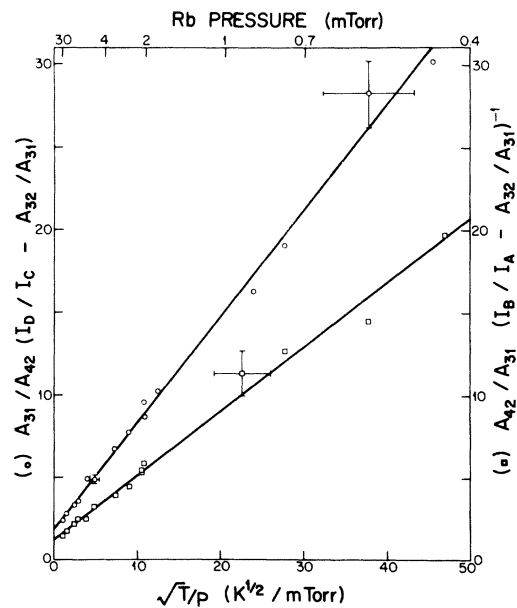


FIG. 3. A plot of the left-hand side of Eqs. (9) and (10) against \sqrt{T}/P . Rough values of Rb vapor pressures are indicated along the abscissa. The error bars are representative of experimental error over the Rb density range.

TABLE I. Cross sections for 2D mixing induced in Rb-Rb collisions (in units of 10^{-13} cm^2).

Collisional partners	2D splitting ΔE (cm^{-1})	Source	Q_{34} ${}^2D_{3/2} \rightarrow {}^2D_{5/2}$	Q_{43} ${}^2D_{3/2} \leftarrow {}^2D_{5/2}$	$\frac{Q_{34}}{Q_{43}}$	Q_3	Q_4	n^*	$\sigma_g({}^2D)$
Rb($6{}^2D$) + Rb($5{}^2S$)	2.26	Hill <i>et al.</i> ^a		1.0 ± 0.6			3.8 ± 0.6	4.68	0.89
Rb($7{}^2D$) + Rb($5{}^2S$)	1.51	This work	3.0 ± 0.5	1.8 ± 0.3	1.65	1.9 ± 0.6	0.7 ± 0.2	5.67	2.0
Rb($8{}^2D$) + Rb($5{}^2S$)	1.01	Glódz <i>et al.</i> ^b	8.1 ± 1.6	5.5 ± 1.1	1.47	3.5 ± 2.2	2.8 ± 2.9	67	4.0
Rb($9{}^2D$) + Rb($5{}^2S$)	0.70	Gouand <i>et al.</i> ^c	7.0 ± 3.0			0.8 ± 0.3		7.66	7.1

^aReference 20.^bReference 9.^cReference 21.

temperatures, the sensitivity calibration of the two detection and counting channels, and the values of the lifetimes and the Einstein A coefficients. The errors assigned to the cross sections Q_3 and Q_4 are correspondingly larger since, as may be seen in Eqs. (9) and (10), their values are derived from Q_{34} and Q_{43} .

As has been pointed out previously,⁹ the excitation transfer process induced in resonant alkali-alkali collisions result from a long-range interaction as manifested by the large cross sections. It is expected that the cross sections should vary inversely with ΔE , the fine-structure separation, though it has been reported for more highly excited states that, at $\Delta E \leq 1 \text{ cm}^{-1}$, there is not much variation.³ It is thus not surprising that the $8D$ and $9D$ cross sections are equal within the stated error, while the $6D$ and $7D$ cross sections decrease with increasing ΔE . In the absence of relevant calculations there are no theoretical values with which the experimental results could be compared. On the other hand, they are comparable to the geometrical cross section¹⁹

$$\sigma_g = \left(\frac{1}{2}\right) \pi a_0^2 n^{*2} [5n^{*2} + 1 - 3l(l+1)], \quad (11)$$

where $a_0 = 0.529 \text{ \AA}$ is the Bohr radius, $l = 2$ for nD states and n^* is the effective quantum number. In their discussion of alkali-alkali collisions, Hugon *et al.*²² showed that their experimental quenching cross sections for Rb nS and $nD_{3/2}$ states were of the same order as the geometrical cross section. Since the $7{}^2D$ states are relatively well separated from other Rb states, Hugon's quenching cross sections may be considered approximately equivalent to our $Q_{34} + Q_3$, the sum of which is close to σ_g , indicating good consistency in the magnitudes of the resonant cross sections for Rb atoms excited to intermediate-energy states.

The experimental data for mixtures of Rb with He, Ne, and Ar are presented in Fig. 4 as plots of Eqs. (9) and (10) in relation to \sqrt{T}/P , where in this case P represents the pressures of the noble gases. Here the plots are also linear except for a few readings taken at the lowest Ar and Ne pressures below 4 mTorr. Since the gas pressures were measured with a trapped McLeod gauge, it is possible that at the very low pressures the heavier gases encountered some difficulty in diffusing into

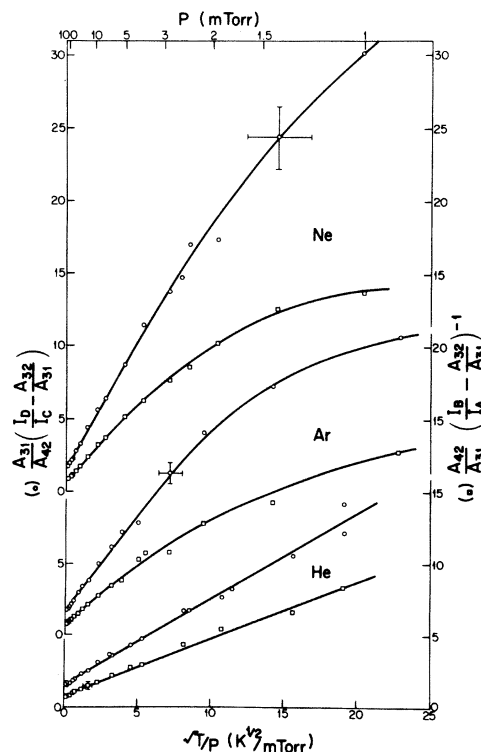


FIG. 4. Plots of the left-hand sides of Eqs. (9) and (10) against \sqrt{T}/P for Ne, Ar, and He. Rough values of gas pressures are indicated along the abscissa. The error bars are representative of experimental error over the range of noble-gas densities.

TABLE II. Cross sections for 7^2D mixing induced in collisions with noble gases (in units of 10^{-14} cm²).

Collision partners	Q_{34} ($^2D_{3/2} \rightarrow ^2D_{5/2}$)	Q_{43} ($^2D_{3/2} \leftarrow ^2D_{5/2}$)	$\frac{Q_{34}}{Q_{43}}$	Q_3	Q_4	Q (Theor.) (Ref. 7)
Rb-He	8.8 ± 1.3	5.8 ± 0.9	1.51	1.1 ± 0.3	0.3 ± 0.1	7.5
Rb-Ne	6.5 ± 1.0	4.0 ± 0.6	1.62	0.2 ± 0.1	0.2 ± 0.1	
Rb-Ar	10.4 ± 1.6	6.9 ± 1.0	1.50	0.1 ± 0.1	0.5 ± 0.5	10

the gauge reservoir against a comparable pressure of Hg vapor with the result that the pressure indicated by the gauge was lower than the actual gas pressure in the cell. Helium, which has a very long mean-free path, does not exhibit this low-pressure effect and shows linear behavior down to a pressure of 1 mTorr. The contribution of Rb-Rb collisions to the observed excitation transfer was estimated to be less than 2% and all the data were corrected appropriately. The excitation transfer and quenching cross sections calculated from the slopes and intercepts in Fig. 4 are listed in Table II. The cross sections are significantly smaller than those for Rb-Rb collisions, in agreement with Omont's calculations⁶ and with experimental measurements pertaining to higher D and F energy levels^{3,4}; few measurements of 2D mixing cross sections for $n < 9$ have been reported and most theoretical work relates also to more highly excited states. A useful comparison may be made with the predictions of Hahn's model for collisions with He and Ar,⁷ and slight extrapolations of the curves in his Fig. 2 produce values in good agreement with those quoted in Table II. It is also apparent that the 2D mixing cross sections increase from Ne to He to Ar. The same ordering of cross sections has been observed in a study of collisional l mixing in sodium,² where it was pointed out that there was a correlation between the relative sizes of the mixing cross sections and of electron scattering lengths of Ne, He, and Ar. Good correlation has also been reported between the electron scattering cross sections and cross sections for resonance 2P mixing in K, Rb, and Cs, for all the noble-gas atoms.²³ Accordingly, the results of this investigation give further support to the view that the excitation transfer process can be regarded as a low-energy scattering phenomenon involving the alkali valence electron. The cross sections Q_{34} and Q_{43} are es-

timated to be accurate within an error of $\pm 15\%$, arising mainly from pressure measurements and, as before, from sensitivity calibration. All the cross sections are subject to uncertainties associated with the calculated transition probabilities. On the other hand, it appeared that the noble-gas cross sections were not noticeably affected by contributions from Rb-Rb collisions. This was verified by carrying out fluorescent intensity measurements over a range of Rb vapor pressures varying by a factor of 4, with no discernible differences in the resulting cross sections. The fluorescent light was also checked for the presence of polarization and was found to be almost depolarized, the small residual effect being most probably instrumental in origin.⁹ Effects due to stimulated emission induced by blackbody radiation²⁴ were deemed to be insignificant because of the relatively large energy separation of the 7^2D levels from other excited states.

According to the principle of detailed balancing

$$\frac{Q_{34}}{Q_{43}} = \frac{g_4}{g_3} \exp\left(\frac{-\Delta E}{kT}\right), \quad (12)$$

where $g_4=6$ and $g_3=4$ are the statistical weights of the $^2D_{5/2}$ and $^2D_{3/2}$ states, respectively. Since $\Delta E \ll kT$, the predicted ratio should equal 1.5. That the ratios of the measured cross sections agree with this value within a smaller margin than the quoted experimental error may be taken as an indication of the internal consistency of the results and of the accuracy of the relative if not absolute values of the cross sections.

ACKNOWLEDGMENT

This work was supported by the National Sciences and Engineering Research Council of Canada.

- *On leave from Nicholas Copernicus University, Toruń, Poland.
- ¹R. Biraben, K. Beroff, G. Grynberg, and E. Giacobino, *J. Phys. (Paris)* **40**, 519 (1979).
- ²T. F. Gallagher, S. A. Edelstein, and R. M. Hill, *Phys. Rev. A* **15**, 1945 (1977).
- ³M. Hugon, F. Gounand, P. R. Fournier, and J. Berlande, *J. Phys. B* **12**, 2707 (1979).
- ⁴M. Hugon, F. Gounand, P. R. Fournier, and J. Berlande, *J. Phys. B* **13**, 1585 (1980).
- ⁵E. de Prunelé and J. Pascale, *J. Phys. B* **12**, 2511 (1979).
- ⁶A. Omont, *J. Phys. (Paris)* **38**, 1343 (1977).
- ⁷Y. Hahn, *J. Phys. B* **14**, 985 (1981).
- ⁸P. Münster and J. Marek, *J. Phys. B* **14**, 1009 (1981), and references therein.
- ⁹M. Głodź, J. B. Atkinson, and L. Krause, *Can. J. Phys.* **59**, 548 (1981).
- ¹⁰J. S. Deech, R. Luypaert, and G. W. Series, *J. Phys. B* **8**, 1406 (1975).
- ¹¹C. Tai, W. Happer, and R. Gupta, *Phys. Rev. A* **12**, 736 (1975).
- ¹²P. Pace and J. B. Atkinson, *Can. J. Phys.* **52**, 1635 (1974).
- ¹³E. M. Anderson and V. A. Zilitis, *Opt. Spectrosc.* (USSR) **16**, 211 (1964).
- ¹⁴H. Lundberg and S. Svanberg, *Phys. Lett.* **56A**, 31 (1976).
- ¹⁵J. Marek and P. Münster, *J. Phys. B* **13**, 1731 (1980).
- ¹⁶J. Migdalek and W. E. Baylis, *Can. J. Phys.* **57**, 1708 (1979).
- ¹⁷M. G. Littmann, *Opt. Lett.* **3**, 138 (1978).
- ¹⁸A. N. Nesmeyanov, *Vapor Pressures of the Elements* (Academic, New York, 1963).
- ¹⁹H. Bethe and E. E. Salpeter, *Handb. Phys.* **35**, 88 (1955).
- ²⁰R. H. Hill, Jr., H. A. Schuessler, and B. G. Zollars, *Phys. Rev. A* **25**, 834 (1982).
- ²¹F. Gounand, P. R. Fournier, and M. Hugon, abstracts of contributed papers, *XI International Conference on the Physics of Electronic and Atomic Collisions*, edited by K. Takayanakis and N. Oda (The Society for Atomic Collision Research, Japan, 1979).
- ²²M. Hugon, F. Gounand, and P. R. Fournier, *J. Phys. B* **13**, L109 (1980).
- ²³L. Krause, in *The Excited State in Chemical Physics*, edited by J. W. McGowan (Wiley, New York, 1975).
- ²⁴W. E. Cooke and T. F. Gallagher, *Phys. Rev. A* **21**, 588 (1980).